

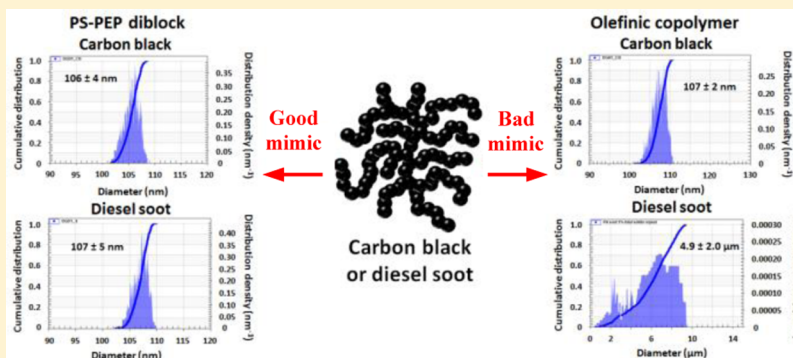
Is Carbon Black a Suitable Model Colloidal Substrate for Diesel Soot?

David J. Gowney,[†] Oleksandr O. Mykhaylyk,[†] Laurence Middlemiss,[†] Lee A. Fielding,[†] Matthew J. Derry,[†] Najib Aragrag,[‡] Gordon D. Lamb,[‡] and Steven P. Armes*,[†]

[†]Department of Chemistry, University of Sheffield, Brook Hill, Sheffield, South Yorkshire S3 7HF, U.K.

[‡]Technology Centre, BP Formulated Products Technology, Whitchurch Hill, Pangbourne RG8 7QR, U.K.

S Supporting Information



ABSTRACT: Soot formation in diesel engines is known to cause premature engine wear. Unfortunately, genuine diesel soot is expensive to generate, so carbon blacks are often used as diesel soot mimics. Herein, the suitability of a commercial carbon black (Regal 250R) as a surrogate for diesel soot dispersed in engine base oil is examined in the presence of two commonly used polymeric lubricant additives. The particle size, morphology, and surface composition of both substrates are assessed using BET surface area analysis, TEM, and XPS. The extent of adsorption of a poly(ethylene-*co*-propylene) (dOCP) statistical copolymer or a polystyrene-*block*-poly(ethylene-*co*-propylene) (PS-PEP) diblock copolymer onto carbon black or diesel soot from *n*-dodecane is compared indirectly using a supernatant depletion assay technique via UV spectroscopy. Thermogravimetric analysis is also used to directly determine the extent of copolymer adsorption. Degrees of dispersion are examined using optical microscopy, TEM, and analytical centrifugation. SAXS studies reveal some structural differences between carbon black and diesel soot particles. The mean radius of gyration determined for the latter is significantly smaller than that calculated for the former, and in the absence of any copolymer, diesel soot suspended in *n*-dodecane forms relatively loose mass fractals compared to carbon black. SAXS provides evidence for copolymer adsorption and indicates that addition of either copolymer transforms the initially compact agglomerates into relatively loose aggregates. Addition of dOCP or PS-PEP does not significantly affect the structure of the carbon black primary particles, with similar results being observed for diesel soot. In favorable cases, remarkably similar data can be obtained for carbon black and diesel soot when using dOCP and PS-PEP as copolymer dispersants. However, it is not difficult to identify simple copolymer–particle–solvent combinations for which substantial differences can be observed. Such observations are most likely the result of dissimilar surface chemistries, which can profoundly affect the colloidal stability.

INTRODUCTION

Diesel engines are widely used in trucks and buses as well as many cars and light-duty vehicles. Their popularity is in large part due to their high thermal efficiency, which leads to lower fuel consumption compared to petrol engines. It is well-known that fuel combustion in diesel engines leads to the production of nitrogen oxides (NO_x) in the exhaust gas, which are harmful to the environment.^{1–6} In the 1990s, diesel engine manufacturers retarded the fuel injection timing in order to meet legislated NO_x emission targets. However, this approach led to an increase in the amount of soot being transferred into the engine oil.⁷ NO_x emission limits have been further tightened within the past 15 years. Automotive manufacturers met these more stringent emissions targets by recirculating the exhaust gas back into the engine; this approach is commonly known as exhaust gas

recirculation (EGR).^{8–11} However, under certain engine operating conditions EGR contributed to the formation of unwanted soot particles within the engine oil.^{12,13} This accumulation of soot within the engine oil leads to higher viscosity, blockage of oil filters, greater engine wear, and sludge formation.¹⁴ Jao et al. reported that soot leads to engine wear via an abrasive wear mechanism. Moreover, the same workers showed that higher levels of abrasive contaminants within the oil inhibits boundary film formation.^{15–17} This excessive build-up of soot particles in engine oil is highly undesirable because it accelerates engine wear, which ultimately leads to lower fuel efficiency and reduced

Received: June 2, 2015

Revised: September 3, 2015

Published: September 5, 2015



Table 1. Summary of Copolymer Composition, Number-Average Molecular Weight (M_n), Weight-Average Molecular Weight (M_w), and Polydispersity (M_w/M_n) As Determined by ^1H NMR Spectroscopy (CDCl_3) and THF GPC (Refractive Index Detector, Polystyrene Standards) Analysis of the Two Commercial Copolymers Used in This Work

copolymer ID	copolymer description	polystyrene content, mol % (^1H NMR, CDCl_3)	M_n (kg mol $^{-1}$)	M_w (kg mol $^{-1}$)	M_w/M_n
dOCP	poly(ethylene- <i>co</i> -propylene) statistical copolymer	N/A	98	146	1.49
PS-PEP	polystyrene- <i>block</i> -poly(ethylene- <i>co</i> -propylene) diblock copolymer	28	117	121	1.04

engine lifetimes.^{18–21} Fortunately, this soot-related wear problem can be mitigated by the addition of various copolymers to engine oil formulations.^{20,22–24} Such copolymers can act as dispersants and confer steric stabilization, thus maximizing the degree of dispersion of the diesel soot. However, genuine diesel soot is prohibitively expensive for optimization studies because it can only be generated by running an engine over an extended period under suboptimal conditions. Thus, various grades of commercial carbon black particles (prepared via gas phase pyrolysis of either hydrocarbon oil or natural gas) have been suggested as cost-effective mimics for diesel soot.^{22,25–28} For example, Clague and co-workers utilized a wide range of techniques, including ^{13}C NMR spectroscopy, IR spectroscopy, atomic emission spectroscopy, thermogravimetric analysis, inverse gas chromatography, transmission electron microscopy (TEM), and X-ray photoelectron spectroscopy (XPS), in order to directly compare both soot extracted from diesel engine oil and also an exhaust soot with various commercial carbon blacks. Although various differences were observed, these authors nevertheless concluded that “there appears to be potential for certain blacks to mimic the aggregation behavior of soots for use in lubrication oils”.²⁷ Similarly, Bezot et al. used static and dynamic light scattering in combination with a reaction limited cluster aggregation mechanism to characterize three types of carbon black in terms of their fractal dimensions.²⁹ However, in a later paper by the same team, only one of these commercial carbon blacks exhibited a similar morphology to that of soot particles isolated from three different drain oils.³⁰ Moreover, Müller et al. compared a commercial carbon black (FR 101 33/D; e.g., Degussa) with soot particulates obtained by running a heavy duty diesel engine under “black smoke” conditions using a range of characterization techniques and concluded that the former material was a poor surrogate for the latter.^{31,32}

In the present study, we examine whether a specific grade of carbon black is a suitable mimic for a particular diesel soot. Initially, various physical properties such as specific surface area, density, particle morphology, and surface composition are determined for both materials using BET surface area analysis, helium pycnometry, TEM, small-angle X-ray scattering (SAXS), aqueous electrophoresis, and XPS. Subsequently, the adsorption of two commercial copolymer dispersants, namely a poly(ethylene-*co*-propylene) (dOCP) statistical copolymer and a polystyrene-*block*-poly(ethylene-*co*-propylene) diblock copolymer (PS-PEP), onto both substrates from *n*-dodecane is examined, both indirectly using a supernatant depletion technique based on UV spectroscopy and also directly via thermogravimetric analysis (TGA). *n*-Dodecane was chosen for these studies because it is comparable to a fully saturated group III base oil, which is widely used in modern engine oils. Finally, relative degrees of dispersion achieved for carbon black and diesel soot when utilizing each copolymer dispersant are assessed using optical microscopy (OM), analytical centrifugation, and SAXS.

EXPERIMENTAL SECTION

Materials. The two copolymers used in this study were commercial products supplied by BP Formulated Products Technology and were used as received. dOCP is a statistical copolymer comprising ethylene and propylene repeat units that also contains a relatively low level (<1 mol %) of aromatic amine functionality. PS-PEP is a linear diblock copolymer with a polystyrene content of 28 mol %, as judged by ^1H NMR spectroscopy;³³ see Table 1 for the corresponding molecular weight and M_w/M_n values. Chloroform and *n*-dodecane were obtained from Fisher Scientific UK Ltd. and were used as received. The carbon black (Regal 250R) was kindly supplied by Cabot Corporation (Billerica, MA). Diesel soot was a gift from BP Formulated Products Technology. This material was generated using a Cambustion diesel particulate generator (DPG) at a loading temperature of 240 °C under the following standard “light duty” test conditions: 1.1 kg h $^{-1}$ fuel flow (standard Euro reference Diesel), 250 kg h $^{-1}$ total flow, and a rate of soot generation of 10 g h $^{-1}$. The soot was then back-blown off the diesel particulate filter (DPF) and collected for analysis. Both colloidal substrates were used as received.

Characterization Techniques. *Gel Permeation Chromatography.* The molecular weight distribution of each copolymer was assessed by gel permeation chromatography (GPC) using THF eluent. The THF GPC setup comprised two 5 μm “Mixed C” 30 cm columns, a Varian 290-LC pump, and a WellChrom K-2301 refractive index detector operating at 950 \pm 30 nm. The THF mobile phase contained 2.0% (v/v) triethylamine and 0.05% (w/w) butylhydroxytoluene (BHT), and the flow rate was fixed at 1.0 mL min $^{-1}$. A series of ten near-monodisperse polystyrene standards ($M_n = 580$ –552 500 g mol $^{-1}$) were used for calibration.

Dynamic Light Scattering. Hydrodynamic diameters were determined by DLS at 25 °C using a Malvern Zetasizer NanoZS model ZEN 3600 instrument equipped with a 4 mW He–Ne solid-state laser operating at 633 nm. Backscattered light was detected at 173°, and the particle size was calculated from the quadratic fitting of the correlation function over 30 runs each of 10 s duration. More specifically, the sphere-equivalent hydrodynamic diameter of the carbon black particles was calculated from the particle diffusion coefficient via the Stokes–Einstein equation, using a solution viscosity of 1.34 cP for *n*-dodecane at 25 °C. All measurements were performed in triplicate, and data were analyzed by cumulants analysis of the experimental correlation function using Dispersion Technology Software version 6.20. Copolymer concentrations of 0.01% (w/v) were utilized in all DLS experiments.

Aqueous Electrophoresis. Zeta potentials were determined for both carbon black and diesel soot particles dispersed in deionized H₂O using the same Malvern Zetasizer Nano ZS instrument described above. The solution pH was initially adjusted to pH 11 in the presence of 1 mM KCl, using 0.1 M NaOH. The solution pH was then manually lowered using either 0.1 or 0.01 M HCl as required.

Transmission Electron Microscopy. Studies were conducted using a Phillips CM100 microscope operating at 100 kV on unstained samples prepared by drying a drop of dilute dispersion (approximately 0.01 wt %) onto a carbon-coated copper grid.

Small-Angle X-ray Scattering. SAXS patterns were acquired at a synchrotron source (Diamond Light Source, station I22, Didcot, UK) using monochromatic X-ray radiation ($\lambda = 0.10$ nm) and a 2D Pilatus 2M detector. A camera length of 10 m provided a q range from 0.014 to 1.85 nm $^{-1}$, where $q = (4\pi \sin \theta)/\lambda$ is the length of the scattering vector and θ is half of the scattering angle. A liquid cell comprising two mica windows (each of 25 μm thickness) separated by a 1 mm

polytetrafluoroethylene spacer was used as a sample holder. In order to avoid sedimentation of the carbon particles on the time scale of the SAXS experiments, the liquid cell was mounted on a continuously rotating stage during data collection. Dawn software developed at Diamond Light Source was used for SAXS data reduction (i.e., integrating, normalization, and background subtraction). Irena SAS macros for Igor Pro³⁴ were used for SAXS data analysis.

Helium Pycnometry. The solid-state densities of the Regal 250R carbon black and genuine diesel soot were determined using a Micrometrics AccuPyc 1330 helium pycnometer at 20 °C.

Surface Area Analysis. BET surface area measurements were performed using a Quantachrome Nova 1000e instrument with dinitrogen gas (mean area per molecule = 16.2 Å²) as an adsorbate at 77 K. Samples were degassed under vacuum at 100 °C for at least 15 h prior to analysis. The particle diameter, d , was calculated using the equation $d = 6/(\rho A_s)$, where A_s is the BET specific surface area in m² g⁻¹ and ρ is the carbon black density in g m⁻³ obtained from helium pycnometry.

UV Spectroscopy. UV spectra were recorded at 20 °C using a PerkinElmer Lambda 25 instrument operating between 200 and 800 nm for dOCP in *n*-dodecane directly, while dilute solutions of PS–PEP diblock copolymer micelles were diluted with an equal volume of chloroform in order to ensure micellar dissolution and hence avoid the problem of UV scattering.³³ A calibration curve was constructed for dOCP in *n*-dodecane and also for PS–PEP in chloroform. The latter copolymer had a molar extinction coefficient of 222 ± 2 mol⁻¹ dm³ cm⁻¹ at 262 nm, which was close to the literature value reported for polystyrene at the same wavelength.³⁵ The supernatant depletion assay was conducted as follows. The desired mass of copolymer (3.0–90.0 mg) was weighed into a glass vial. *n*-Dodecane (5.00 mL) was added to this vial and stirred at 20 °C (Turrax stirrer, 1 min), followed by heating to 110 °C for 1 h. The resulting solution was added to a second glass vial containing carbon black (300.0 mg), stirred (Turrax stirrer, 1 min), sonicated for 1 h, and then placed on a roller mill for 16 h overnight to aid dispersion. The resulting carbon black dispersion was centrifuged for 4 h at 18 000 rpm in a centrifuge rotor that was precooled to 15 °C so as to minimize solvent evaporation. Taking care not to disturb the sedimented carbon black particles, the supernatant was decanted into an empty vial and then analyzed by UV spectroscopy. For PS–PEP micelles, 0.40 mL of this decanted solution was diluted with an equal volume of chloroform to ensure molecular dissolution of the copolymer micelles prior to analysis by UV spectroscopy. The aromatic chromophore at 262 nm corresponding to the polystyrene block in the PS–PEP copolymer was used to quantify the copolymer concentration remaining in the supernatant after exposure to the carbon black, thus enabling the adsorbed amount to be determined by difference. Essentially the same protocol was used for the dOCP, but in this case the aromatic amine chromophore at 292 nm was used for quantification. No chloroform dilution was required in this latter case, since this copolymer does not form micelles in *n*-dodecane. The same analytical protocol was also used for genuine diesel soot, although in this case only 100.0 mg was used in each experiment.

Thermogravimetric Analysis. Analyses were conducted on the two copolymers alone, the pristine carbon black and diesel soot, copolymer-coated carbon black particles and copolymer-coated soot particles. Each sample was heated up to 800 °C under a nitrogen atmosphere at a heating rate of 10 °C min⁻¹ using a Q500 TGA instrument (TA Instruments). The mass loss observed between 300 and 550 °C confirmed complete pyrolysis of both copolymers under these conditions, enabling the remaining incombustible residues to be attributed to either carbon black or diesel soot, respectively.

X-ray Photoelectron Spectroscopy. Studies were conducted on carbon black and genuine diesel soot samples pressed onto indium foil using a Kratos Axis Ultra DLD X-ray photoelectron spectrometer equipped with a monochromatic Al X-ray source ($h\nu = 1486.6$ eV) operating at 6.0 mA and 15 kV at a typical base pressure of 10⁻⁸ Torr. The step size was 1.0 eV for all survey spectra (pass energy = 160 eV). Spectra were typically acquired from at least two separate sample areas. CasaXPS software (version 2.3.15) was used to analyze the spectra,

including background subtraction (using the Shirley algorithm), elemental quantification, and peak deconvolution.

Analytical Centrifugation. Carbon black aggregate diameters were determined using a LUMiSizer analytical photocentrifuge (LUM GmbH, Berlin, Germany) at 20 °C using 2 mm path length polyamide cells. The LUMiSizer is a microprocessor-controlled instrument that employs STEP Technology (space- and time-resolved extinction profiles) allowing the measurement of the intensity of transmitted light as a function of time and position over the entire cell length simultaneously. The progression of these transmission profiles contains information on the rate of sedimentation and, given knowledge of the effective particle density, enables calculation of the particle size distribution. Measurements were conducted on 1.0% w/w carbon black or diesel soot dispersions in *n*-dodecane at 200–4000 rpm. In the present case, the effective particle density is significantly lower than that of either carbon black or diesel soot alone because of the presence of a relatively thick solvated shell of adsorbed copolymer.

RESULTS AND DISCUSSION

Carbon Black and Diesel Soot Characterization. The Regal 250R carbon black used in this work was compared in terms of its particle size, morphology, specific surface area, and surface chemistry to a particular diesel soot. BET surface area analysis yielded 43 m² g⁻¹ for the carbon black particles and 55 m² g⁻¹ for the diesel soot, while helium pycnometry gave densities of 1.89 and 1.94 g cm⁻³, respectively. These data are in sufficiently close agreement to suggest that this particular grade of carbon black may be a useful mimic for diesel soot. Representative TEM images obtained for both carbon black and soot are shown in Figure 1. Analysis of these two images enables

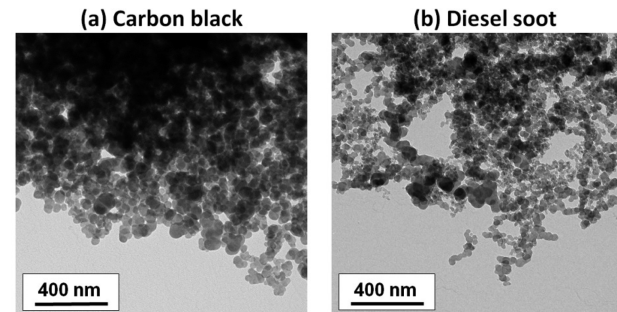


Figure 1. Transmission electron microscopy (TEM) images obtained for (a) carbon black and (b) diesel soot suspensions dried from *n*-heptane. The estimated number-average particle diameters are (a) 70 nm and (b) 50 nm.

number-average diameters of 70 nm for carbon black and 50 nm for genuine soot to be estimated. In a recent related study, we have used SAXS to identify three hierarchical structures for this particular grade of carbon black when prepared as a dispersion in *n*-dodecane.³⁶ Similar structures have been observed in the current study (see later).

The carbon black and diesel soot particles formed stable colloidal suspensions when dispersed in water. Although not necessarily representative of those suspensions formed in *n*-dodecane, such suspensions do enable aqueous electrophoresis studies to be conducted. The variation of both zeta potential and intensity-average particle diameter with solution pH for both colloidal substrates is shown in Figure 2. Carbon black aggregates are highly anionic (−30 to −45 mV) between pH 6 and pH 11. Below pH 6, the gradual reduction in surface charge leads to their progressive aggregation, from an initial characteristic sphere-equivalent diameter of 200 nm in alkaline media to flocs of more

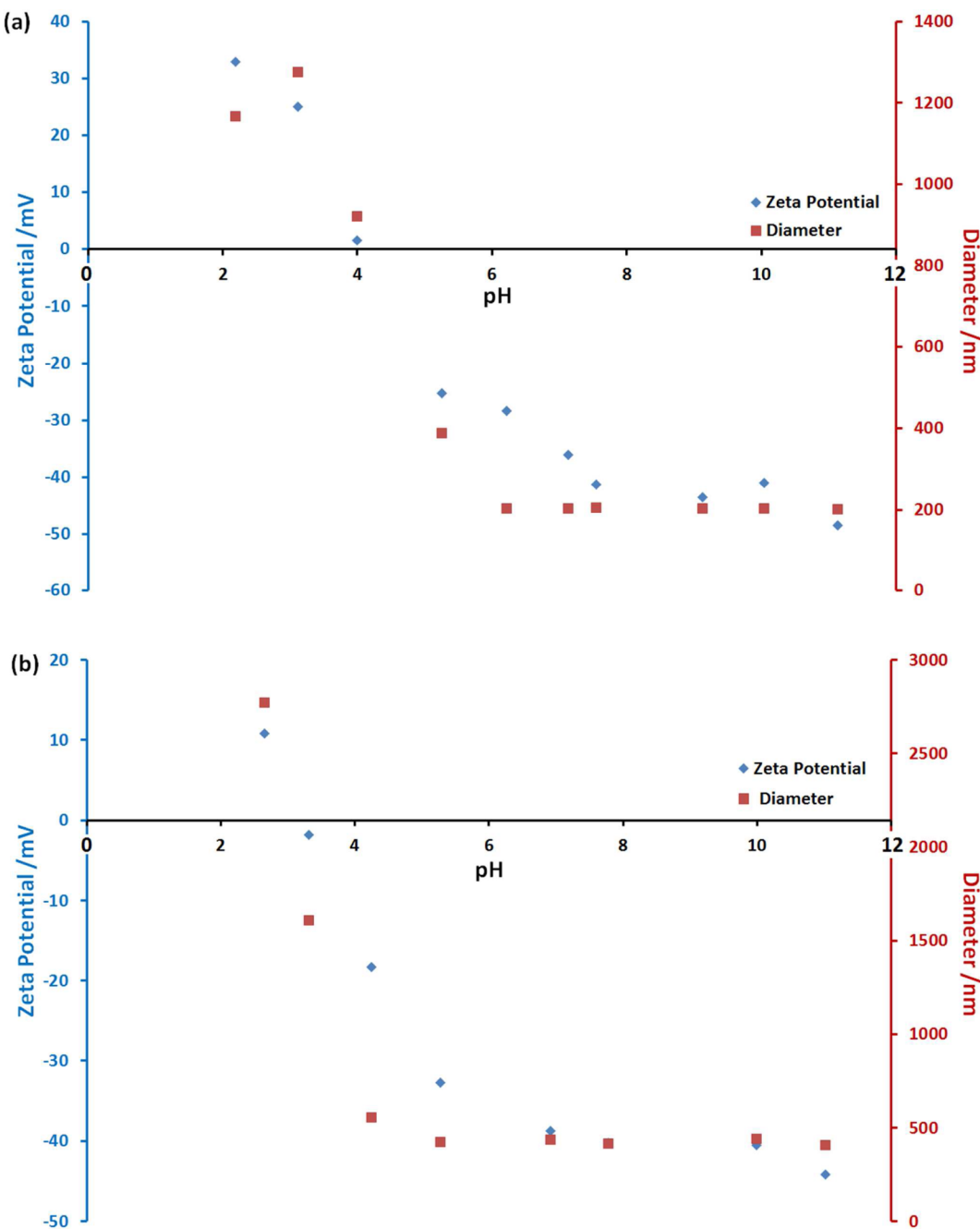


Figure 2. Zeta potential and intensity-average diameter versus pH for dilute (0.002% w/w) aqueous suspensions of (a) carbon black and (b) diesel soot particles at 25°C .

than 800 nm at an isoelectric point (IEP) of approximately pH 4.2 and micron-sized aggregates with appreciable cationic surface charge at pH 2–3. The diesel soot particles exhibit broadly similar behavior, but with some subtle differences. The aggregates formed in alkaline media are somewhat larger, with sphere-equivalent diameters of 400–440 nm and zeta potentials of around -40 mV ; they remain more or less stable from pH 11 to around pH 4, with an isoelectric point at approximately pH 3. Micron-sized aggregates are formed between pH 2 and pH 3.

X-ray photoelectron spectroscopy (XPS) is a well-established surface analysis technique with a typical sampling depth of 2–5 nm.^{37–39} Figure 3 shows the survey spectra and core-line spectra (S 2p and O 1s) recorded for carbon black and diesel soot, respectively. The former substrate contains 98.3 atom %

carbon, 1.1 atom % oxygen, and 0.6 atom % sulfur. In contrast, the latter substrate contains significantly more oxygen (6.3 atom %) but essentially zero sulfur (and 93.7 atom % carbon). As expected,²⁷ examination of the C 1s core-line spectra shows little difference between carbon black and diesel soot (see Supporting Information, Figure S1). These spectra are best fitted using an asymmetric graphitic carbon signal at 284.4 eV plus a shake-up satellite at approximately 291 eV. Unfortunately, this does not allow quantification of the degree of surface functionalization of the carbon black and diesel soot. However, analysis of the O 1s spectra (Figures 3c,d) indicates the presence of at least two surface oxygen species for both carbon black and diesel soot. Following the work of Müller et al.,²⁷ we assign the two main O 1s species to be C=O-C and C=O-H plus a possible minor carbonyl signal

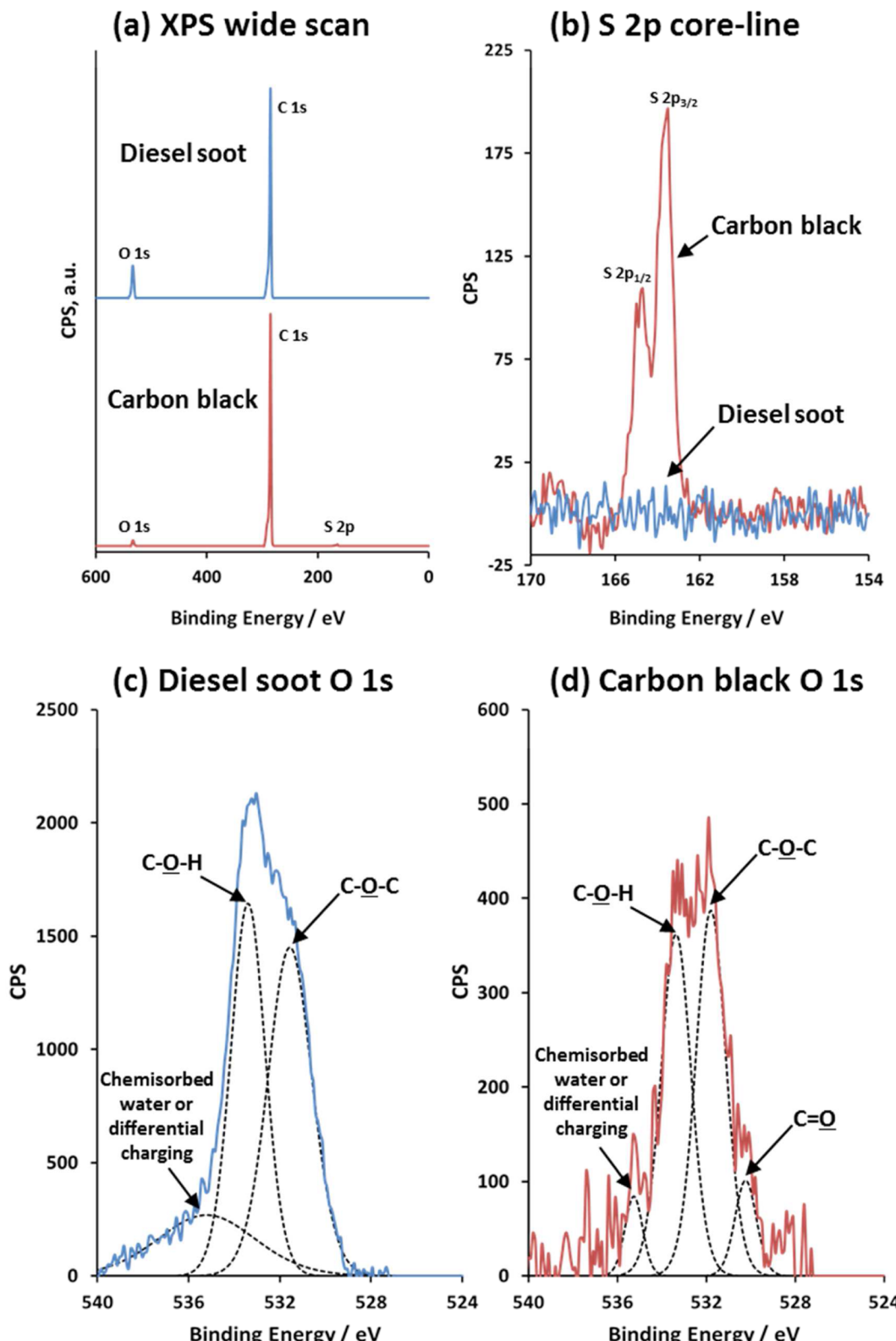


Figure 3. X-ray photoelectron spectra recorded for both carbon black and diesel soot particles: (a) survey spectra, (b) S 2p core-line spectra, (c) peak-fitted diesel soot O 1s core-line, and (d) peak-fitted carbon black O 1s core-line spectra.

contributing to the carbon black spectrum. The latter two species could account for the anionic surface charge observed above pH 7, as indicated by aqueous electrophoresis studies (see Figure 2).

DLS diameters obtained for carbon black and diesel soot particles suspended in *n*-dodecane are comparable, with a slightly

higher intensity-average diameter being observed for the former substrate (see Figure S2). This agrees with TEM studies, which suggest a lower number-average diameter for diesel soot (50 vs 70 nm, see Figure 1). SAXS analyses are also consistent with these observations (see later).

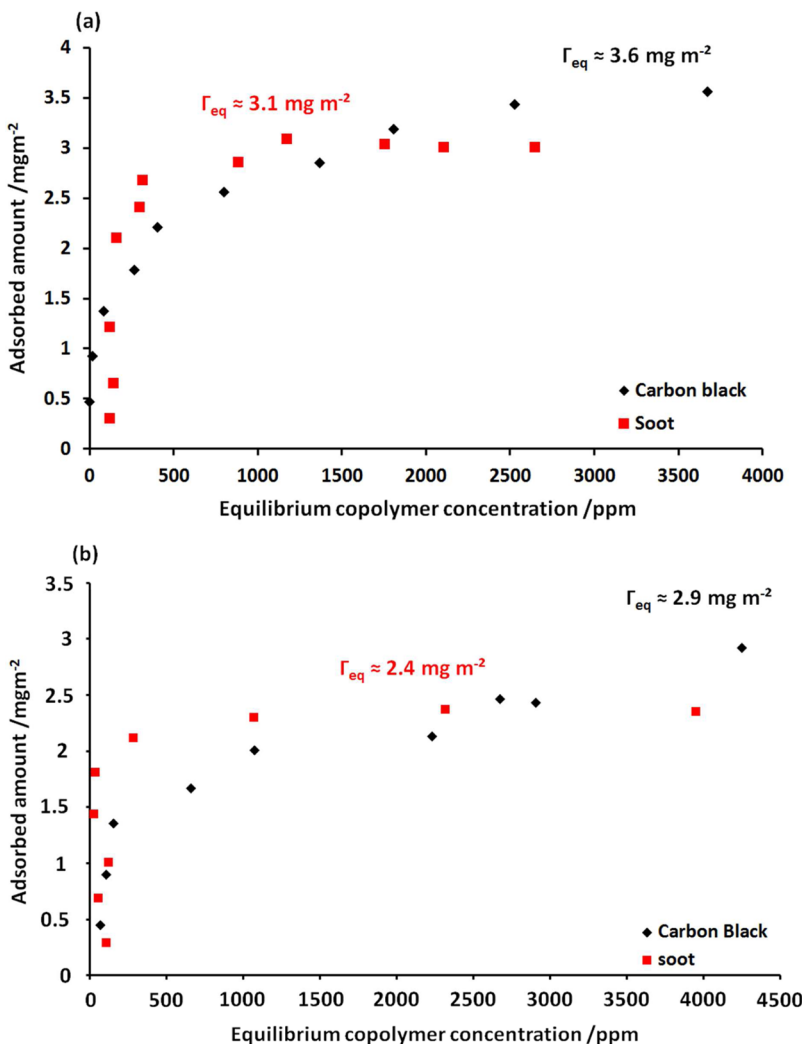


Figure 4. Adsorption isotherms obtained for (a) dOCP and (b) PS-PEP additives adsorbed onto carbon black (black) and diesel soot (red) from *n*-dodecane (after heating to 110 °C for 1 h) at 20 °C, as determined using a UV spectroscopy-based supernatant depletion assay.

Thermogravimetric analysis was used to assess the thermal stabilities of both carbon black and diesel soot on heating under a nitrogen atmosphere (see Figure S3). The former substrate exhibits a somewhat higher thermal stability than the latter, with mass losses of 0.75% and 6%, respectively, being observed at 600 °C. Above 600 °C, substantial mass loss was observed for the diesel soot. However, this does not adversely affect the assessment of copolymer adsorption using this method, since complete pyrolysis of both copolymers used in this study is observed between 300 and 550 °C under the same conditions (see below).

Copolymer Characterization. The two copolymers employed in this work were characterized using THF GPC and ¹H NMR (CDCl_3) (see Table 1). These copolymers were selected because they represent two important classes of copolymer dispersant used for commercial engine oil formulations. PS-PEP is a polystyrene-block-poly(ethylene-co-propylene) diblock copolymer dispersant which forms polystyrene-core micelles in selective solvents such as *n*-alkanes (or engine oil). Such micelles adsorb intact onto carbon black particles to confer steric stabilization at 20 °C, as discussed in our earlier study.³³ However, it is not clear whether micelle adsorption also occurs at typical engine operating temperatures of 90–100 °C. In contrast, dOCP is a poly(ethylene-co-propylene)

statistical copolymer containing a relatively low level of aromatic amine functionality.

Copolymer Adsorption Isotherms on Carbon Black and Diesel Soot. Isotherms were constructed for the adsorption of each copolymer onto both carbon black and soot from *n*-dodecane using a supernatant depletion assay based on UV absorption spectroscopy, after centrifugal sedimentation of the carbon black particles (see Figure 4). *n*-Dodecane was selected instead of an engine base oil because the latter solvent invariably contains UV-absorbing species, which renders UV spectroscopy analysis problematic. For PS-PEP, the polystyrene block acts as a convenient UV chromophore, since it gives rise to a strong signal at 262 nm.⁴⁰ In the case of dOCP, a strong absorbance at 292 nm resulting from its aromatic amine functionality provides a suitable UV signal. It is well-known that PS-PEP forms polystyrene-core micelles in *n*-alkanes.^{22,41,42} Hence, the supernatant assay cannot be performed directly in such solvents because of light scattering at shorter wavelengths. Instead, the supernatant solution obtained after centrifugation of the carbon particles is diluted with an equal volume of chloroform. Growney and co-workers³³ have shown that addition of this good solvent for the polystyrene chains causes micellar dissociation, producing molecularly dissolved copolymer chains that are suitable for the UV assay. Addition of chloroform was not required for the

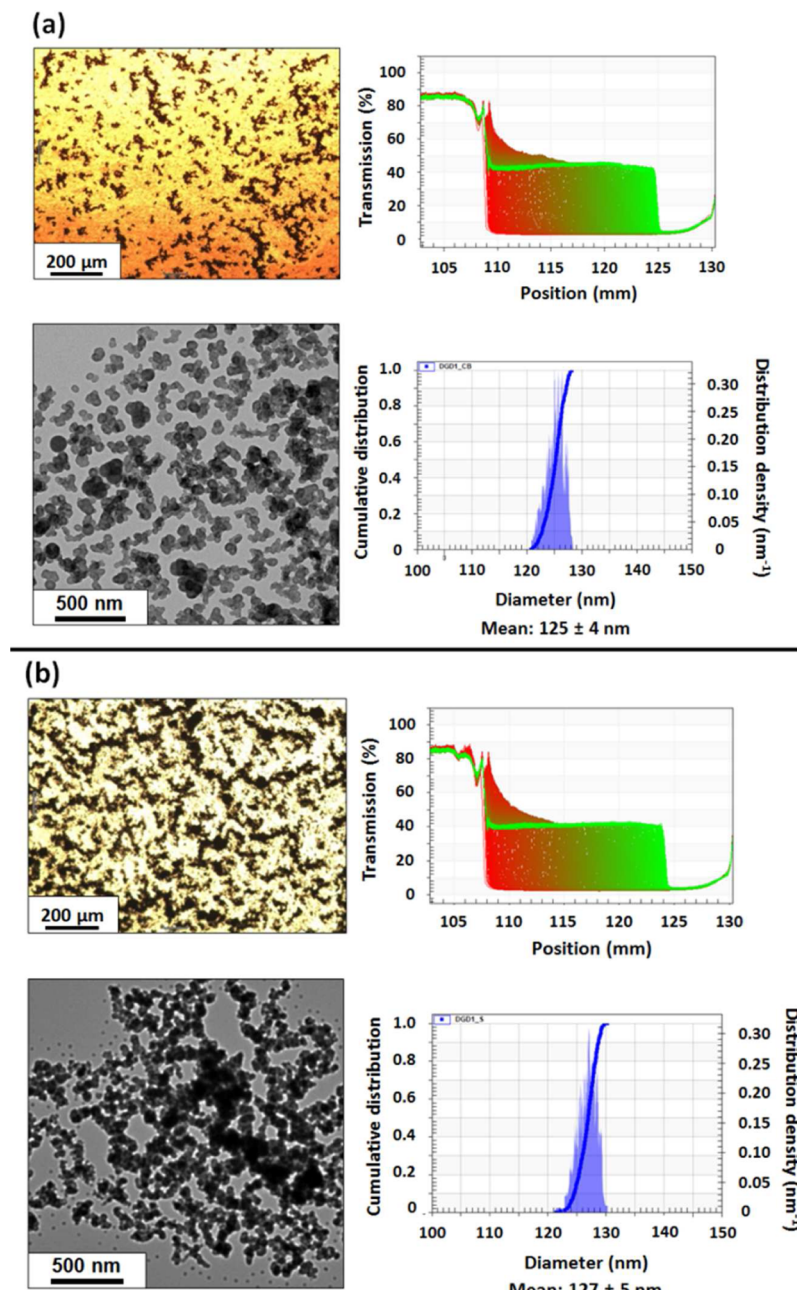


Figure 5. Optical microscopy images, TEM images, and LUMiSizer raw profile plots and volume-average particle size distributions obtained at 20 °C for (a) carbon black particles dispersed in *n*-dodecane and (b) diesel soot particles dispersed in *n*-dodecane. In each case 10% PS–PEP copolymer by mass was utilized relative to the colloidal substrate.

dOCP, since this copolymer does not form micellar structures in *n*-dodecane. Langmuir-type adsorption is observed for both copolymers, with the plateau region indicating monolayer coverage.⁴³ Such behavior is expected for adsorption of individual copolymer chains, but it is worth emphasizing that PS–PEP is actually adsorbed in the form of micelles.³³ Thus, it seems rather counterintuitive that PS–PEP actually has a *lower* maximum adsorbed amount ($\Gamma = 2.4 \text{ mg m}^{-2}$) than the latter ($\Gamma = 3.1 \text{ mg m}^{-2}$). One explanation for this apparent discrepancy is that the dOCP copolymer forms intermolecular aggregates in solution, rather than molecularly dissolved chains. Indeed, this is consistent with the observed sedimentation of dOCP during centrifugation (see below).

Thermogravimetric analysis (TGA) was also used to quantify the extent of adsorption of each copolymer on the surface of

carbon black and diesel soot particles from *n*-dodecane. Minimal mass loss occurred on heating such particles to 550 °C under an inert atmosphere (see Figure S3). In contrast, both copolymers were fully pyrolyzed under these conditions (see inset thermograms in Figure S4). Thus, pyrolysis of the copolymer-coated carbon black and soot particles (isolated as compacted sediments after centrifugation) allows the adsorbed amount of copolymer to be determined directly. A series of thermograms are shown in Figure S4. Higher mass losses are observed between 300 and 550 °C as the initial copolymer concentration is gradually increased. Initially, similar adsorption affinities are observed for each copolymer on both carbon black and diesel soot, while the maximum adsorbed amount (corresponding to monolayer coverage) was higher for the latter substrate. Adsorption isotherms

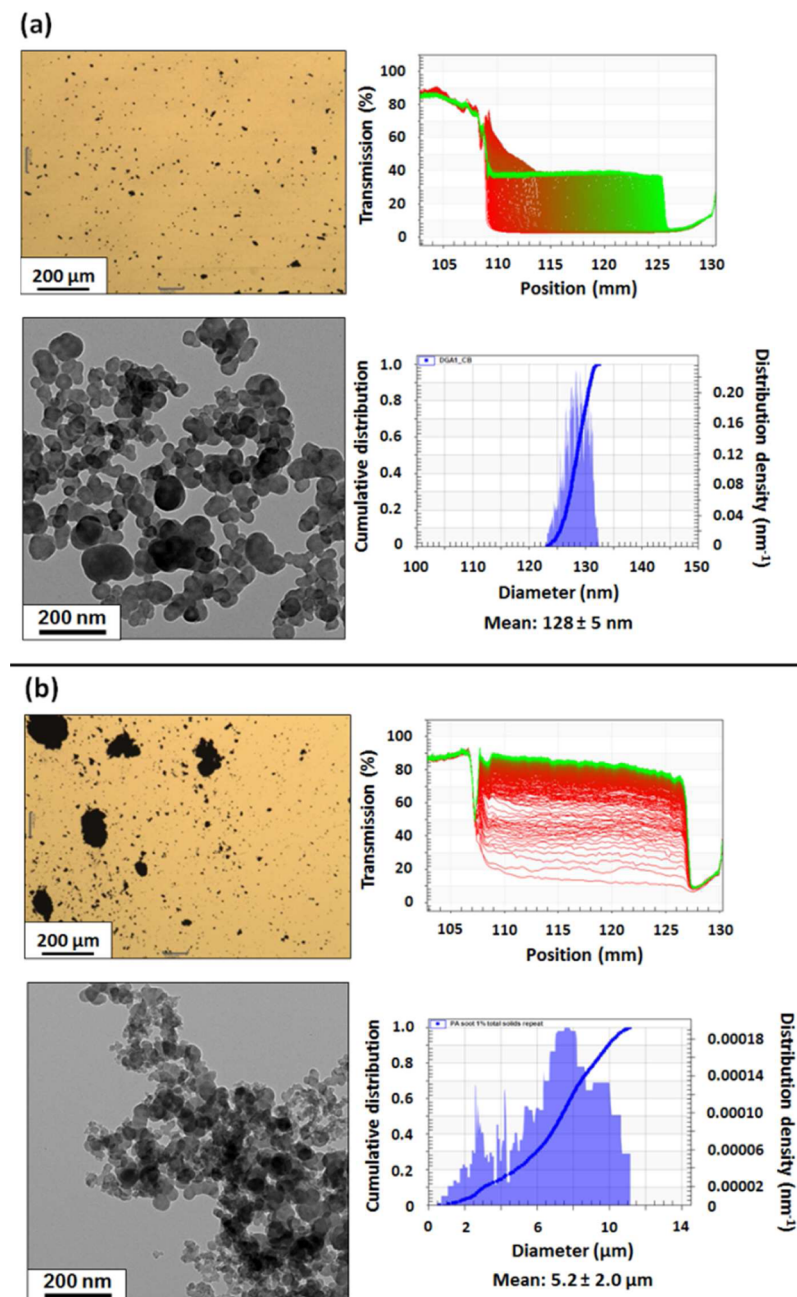


Figure 6. Optical microscopy images, TEM images, and LUMiSizer raw profile plots and volume-average particle size distributions obtained at 20 °C for (a) carbon black particles dispersed in *n*-dodecane and (b) diesel soot particles dispersed in *n*-dodecane. In each case 10% dOCP copolymer by mass was utilized relative to the colloidal substrate.

constructed using each technique for both copolymers adsorbed onto soot are shown in Figure S5. When assessed using TGA, the apparent adsorbed amount continues to increase beyond the monolayer coverage value indicated by UV spectroscopy. However, control experiments conducted in the absence of any carbon black (or diesel soot) confirm that both copolymers are partially sedimented under the centrifugation conditions used for the adsorption studies. This observation is understandable for the PS–PEP copolymer because TEM, DLS and SAXS studies indicate micelle formation in *n*-dodecane.³³ It is perhaps less clear why the dOCP copolymer should form aggregates in solution, but this may be related to its low degree of diphenylamine functionality, which is likely to lead to intermolecular π – π stacking interactions.⁴⁴ In view of these observations, TGA

should be reliable below (and up to) monolayer coverage because under these conditions there is essentially no excess copolymer in the supernatant. However, the adsorbed amount tends to be *overestimated* by this technique when either copolymer is present in excess, since non-adsorbed copolymer is sedimented along with the carbon black (or diesel soot) particles. For the same reason, the UV supernatant depletion assay necessarily *underestimates* the adsorbed amount of copolymer when working above monolayer coverage. Although this technical problem is an important caveat, the TGA data nevertheless confirm a higher equilibrium adsorbed amount for dOCP compared to PS–PEP for both substrates (see Table S1).

Relative Degrees of Dispersion of Carbon Black and Diesel Soot in *n*-Dodecane. In principle, a smaller apparent

particle size indicates a higher degree of dispersion for the carbon black or diesel soot particles in *n*-dodecane. In this context, there are two particle size regimes of interest. *Micron-sized* agglomerates (or mass fractals⁴⁵) are readily visualized by optical microscopy.⁴⁶ Figure 5 shows representative optical microscopy images obtained for both carbon black and diesel soot particles when using PS–PEP copolymer as a dispersant (at 10% w/w based on the mass of particles). Clearly, similar degrees of dispersion are observed for each substrate. Moreover, TEM images recorded for the *submicron-sized* populations of carbon black and diesel soot particles are also comparable. In principle, analysis of these submicron-sized populations can be achieved for both colloidal substrates using analytical centrifugation (LUMi-Sizer instrument).^{47–50} In practice, this technique requires an accurate particle density. However, determining this parameter can be problematic for sterically stabilized particles, particularly for thick stabilizer layers on relatively small particles. We have recently calculated an effective particle density of 0.91 g cm^{−3} for PS–PEP-coated carbon black particles in *n*-dodecane.⁵⁰ This density is significantly lower than that of carbon black alone (1.89 g cm^{−3}), which leads to a substantial correction to the volume-average particle diameter determined by analytical centrifugation. In the absence of any other data, we have used the above effective particle density for the dOCP-coated carbon black particles and also for both types of copolymer-coated diesel soot particles. The volume-average particle size distributions determined for PS–PEP-coated carbon black and diesel soot particles using this effective particle density are shown in Figure 5. This analysis was conducted at a concentration of 1.0% w/w carbon black (based on solvent), since higher concentrations tend to give artificially low volume-average diameters due to hindered settling and multiple scattering⁴⁸ (see Figure S6). Remarkably similar volume-average particle diameters (125 nm vs 127 nm) are calculated, which suggests that carbon black is a useful model substrate for understanding the behavior of diesel soot, at least for this particular copolymer under these conditions.

In Figure 6, the equivalent optical microscopy and TEM images obtained for dOCP-coated carbon black (or diesel soot) particles are presented. However, in this case the diesel soot is substantially more aggregated than carbon black particles prepared under the same conditions. This conclusion is reinforced by the analytical centrifugation data, which report an apparent volume-average particle diameter of 5.2 μm for the diesel soot particles but only 128 nm for the carbon black particles. Thus, for this particular copolymer at this specific concentration, it is clear that carbon black is a poor mimic for the behavior of diesel soot. These differences are most likely the result of a specific acid–base interaction between the diphenylamine-functionalized dOCP copolymer and the carboxylic acid-rich surface of the diesel soot, which leads to bridging flocculation rather than steric stabilization.

SAXS Analysis. It is well-known that the morphology of carbon black (and diesel soot) can be described as a complex hierarchy composed of five structures/levels: (i) fractal agglomerates at the micron length scale, (ii) aggregates and (iii) primary particles at the nanometer scale, (iv) subunits (a turbostratic structure comprising graphite-like layers arranged in nonaligned basal planes) at the sub-nanometer scale, and finally (v) graphite-like carbon layers at the atomic scale.^{51–55} The first three structures can be analyzed by SAXS/USAXS (ultrasmall-angle X-ray scattering) and are shown in cartoon format in Figure 7, while the remaining two structures can be characterized using wide-angle X-ray scattering (WAXS). The primary

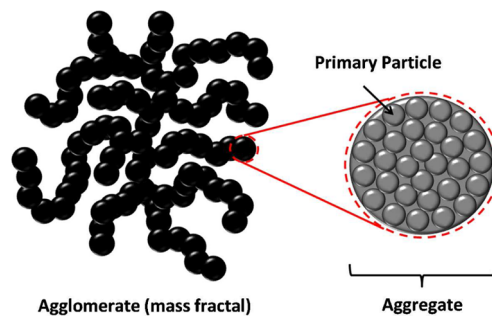


Figure 7. Schematic cartoon illustrating the three structural morphologies identified for carbon black and diesel soot via SAXS analysis. The rough surface fractal nature of the primary particles (and aggregates) is not shown in this cartoon.

particles are fused together to form aggregates that are considered to be unbreakable via dispersion processes,⁵⁴ but the larger hierarchical structures can be affected by the processing conditions.^{51,56,57} Thus, SAXS/USAXS measurements are often employed for characterization of carbon black/diesel soot in order to obtain structural information regarding the organization of the aggregated particles.^{54,57,58} In this context, the unified Guinier plus power law approach proposed by Beaucage is commonly employed,^{59–61} since it enables an arbitrary number of interrelated structural features at various length scales to be described.^{54,62} The scattering profile, $I(q)$, is decomposed into the scattering intensity arising from each structural element comprising the hierarchical structures. It can be expressed analytically as follows:

$$I(q) \cong \sum_{i=1}^N \left[G_i \exp\left(-\frac{q^2 R_{g,i}^2}{3}\right) + B_i \exp\left(-\frac{q^2 R_{g,i+1}^2}{3}\right) \times \left(\frac{[\text{erf}(qk_i R_{g,i}/\sqrt{6})]^3}{q} \right)^{P_i} \right] S_i(q) \quad (1)$$

where N is the number of structural elements, and the scattering intensity originating from each structural element (the expression enclosed by the square brackets) is represented as the sum of two components describing the Guinier and power laws, respectively. G_i is the Guinier pre-exponential factor of the i th structural element, and B_i is a prefactor of the power-law scattering. $R_{g,i}$ and $R_{g,i+1}$ are radii of gyration of a large-scale structure and a small-scale substructure, respectively. The exponent term associated with $R_{g,i+1}$ provides a high q cut-off for the power law component, which is incorporated into eq 1 in order to describe scattering from a system with inter-related multiscaling features. This factor is commonly used to describe mass fractals.^{34,60} If it is not required, the exponent term is assumed to be unity. P_i is a scaling exponent of the power law assigned to the larger structure $R_{g,i}$. Generally, the numerical value of the exponent enables the structural morphology to be classified. For mass fractals $P_i < 3$, for surface fractals $3 < P_i < 4$, for Porod's law (smooth surface with a sharp interface) $P_i = 4$, and for diffuse interfaces $P_i > 4$ (negative deviation from Porod's law). k_i is an empirical constant that is either unity for steep power law decays ($P_i > 3$) or equal to 1.06 for mass fractals ($1.5 < P_i < 3$).⁶⁰ Weakly correlated particles can also be considered using eq 1 by incorporating a structure factor, $S_i(q)$,^{61,63} which comprises a damped spherical correlation of colloidal particles:

$$S_i(q) = [1 + \eta f(qR_{c,i})]^{-1} \quad (2)$$

where $f(qR_{c,i}) = 3[\sin(qR_{c,i}) - qR_{c,i} \cos(qR_{c,i})]/(qR_{c,i})^3$ is the form factor for spherical interactions correlated over a distance R_c and η describes the degree of correlation, which is assumed to be weak if $\eta < 3$. If no correlations are present for the i th structural element/level, then $S_i(q) = 1$. The multi-level unified fit, eq 1, is implemented as a routine in the SAXS data analysis software Irena SAS macros for Igor Pro.³⁴

Three hierarchical structures can be identified in the SAXS pattern recorded for the original carbon black dispersed in *n*-dodecane (Figures 8 and 9, low SAXS pattern). By analogy

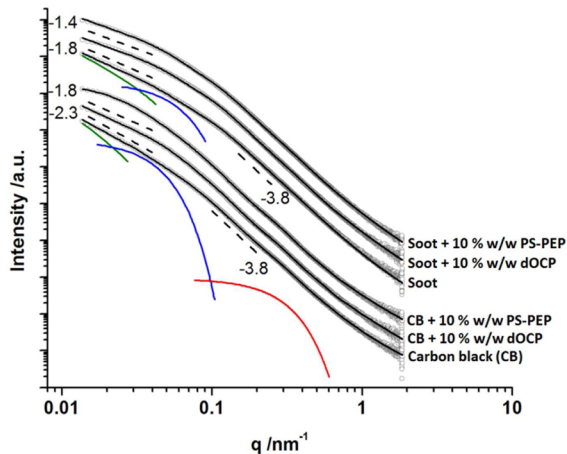


Figure 8. Representative SAXS patterns recorded for 1.0% w/w carbon black or diesel soot dispersions in *n*-dodecane in the absence and presence of two commercial copolymer dispersants (dOCP and PS-PEP; 10.0% w/w loading based on carbon black or diesel soot particles). The lower group of patterns was obtained for carbon black particles, and the upper group was obtained for diesel soot. Dashed lines indicate power law gradients for the scattering intensity. Solid black lines indicate multi-level unified fits to the data. Colored lines indicate unified fits to the mass fractals (green) and the Guinier components of the unified fits to both the agglomerates (blue) and the primary particles (red).

with previous work,⁵⁸ the SAXS intensity gradient of -2.3 for $q < 0.03 \text{ nm}^{-1}$ is associated with mass fractals formed by carbon black aggregates and the corresponding gradient of -3.8 for $0.1 \text{ nm}^{-1} < q < 0.2 \text{ nm}^{-1}$ is assigned to surface fractals of the aggregates. Primary particles can be clearly identified as an upturn in SAXS intensity at $q \sim 0.3 \text{ nm}^{-1}$ via a Porod plot (Figure 9, low pattern). Thus, SAXS patterns obtained for the original carbon black dispersion in *n*-dodecane can be interpreted as a superposition of scattering from primary particles (level 3), aggregates of these primary particles (level 2), and mass fractals of the aggregates (level 1) (Table 2). Structural characteristics of the carbon black can be determined by fitting the unified model to the scattering patterns (eq 1). A multi-level unified fit approach described in a previous study⁵⁴ has been employed for the SAXS analysis in this work. The SAXS pattern for the initial dispersion of carbon black in *n*-dodecane is reasonably well described by this model (see the lowest patterns in Figures 8 and 9). The mean primary particle size, $2R_{g,3}$, is 14.2 nm (Table 2, level 3), which is comparable to data reported in other studies.^{51,54,58} The aggregate size, $2R_{g,2} = 105$ nm (Table 2, level 2) corresponding to particle diameter 81 nm ($(2R_{g,2}/3/5)^{1/2}$) is also within the size range observed previously.⁵¹ The power law exponent for these aggregates, P_2 , is equal to 3.8 (Table 2). Since this value is just below 4.0, it suggests that the primary particles comprising these aggregates have a slightly rough surface. It is usually found that

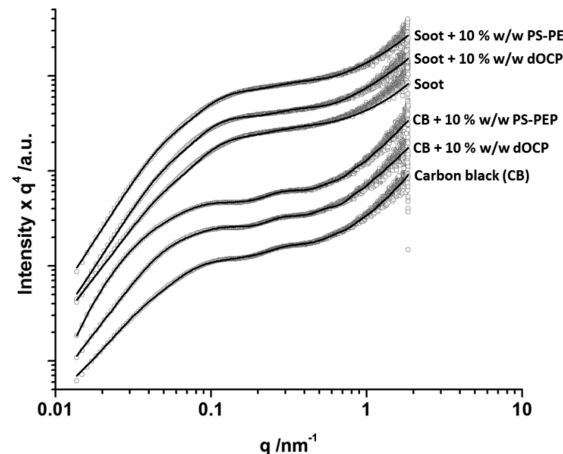


Figure 9. Porod plots for representative SAXS patterns recorded for 1.0% w/w carbon black or diesel soot dispersions in *n*-dodecane in the absence and presence of two commercial copolymer dispersants (dOCP and PS-PEP; 10.0% w/w loading based on carbon black or diesel soot particles). The lower group of patterns was obtained for carbon black particles, and the upper group was obtained for diesel soot. Solid lines indicate multilevel unified fits to the experimental data.

Table 2. Calculated Parameters for Three Hierarchical Structures (Levels) Derived from Multi-Level Unified Fits to the Experimental SAXS Patterns Recorded for 1.0% w/w Carbon Black or Diesel Soot Dispersion in the Absence and Presence of Two Commercial Copolymer Dispersants (DOCP and PS-PEP)^a

sample description	level 1 (fractals)		level 2 (aggregates)		level 3 (primary particles)		
	P_1	$2R_{g,2}$	P_2	$2R_{g,3}$	P_3	$R_{c,3}$	η_3
carbon black particles	2.7	105	3.8	14.2	1.7	20	2.2
carbon black particles plus 10% w/w dOCP	2.0	76	4.2	13.0	2.2	22	2.3
carbon black particles plus 10% w/w PS-PEP	2.3 ^b	102	4.0	13.6	2.0	22	2.2
diesel soot particles	2.1	74	3.8	14.0 ^c	1.8		
diesel soot particles plus 10% w/w dOCP	1.7	70	4.1	14.0 ^c	2.4		
diesel soot particles plus 10% w/w PS-PEP	1.7	71	4.0	14.0 ^c	2.2		

^a P_1 , P_2 , or P_3 is the relevant power law exponent, $2R_{g,2}$ or $2R_{g,3}$ is the size of the structural element in nm, $R_{c,3}$ is the correlation distance in nm, and η is the corresponding degree of correlation. Errors in the fitted parameters shown in this table are within a unit of the last digit of the values given. ^bA radius of gyration of the agglomerate was incorporated into the fitting model, $R_{g,1} = 340$ nm. ^cThis parameter was fixed during SAXS data fitting.

the power law exponent for such aggregates ranges from 3.4 to 4.0,^{51,54,55,57,62} suggesting that the electron density distribution at the primary particle surface can vary according to the synthesis method and processing conditions. The power law exponent of the mass fractals formed by the aggregates (Table 2, level 1) corresponds to a fractal dimension D_m (or P_1) of 2.7. A similar fractal dimension was observed for diesel soot dispersed in acetone.⁵⁸ Thus, the structural morphology of the carbon black particles dispersed in *n*-dodecane can be described as relatively compact mass fractals (Figure 1). It was also found that incorporating an appropriate structure factor into the model produced a better fit to the SAXS pattern recorded for the

primary particles (level 3). More detailed analysis revealed a weak correlation between the primary particles ($\eta_3 < 3$, see Table 2). The power law exponent calculated for the primary particles, P_3 , is also given in Table 2. This parameter is based on the scattering at high q . However, it is difficult to interpret such exponents as this region of the scattering pattern is influenced by excess scattering from a smaller hierarchical carbon structure (subunits of $\sim 1.5\text{--}2.0\text{ nm}$) and also by internal inhomogeneities within carbon particles comprising both crystalline and amorphous phases.^{52,54,62}

The model incorporating three hierarchical levels utilized for the carbon black particles also produced a reasonably good fit to the SAXS patterns recorded for a 1.0% w/w diesel soot dispersion in *n*-dodecane (Figures 8 and 9). However, inspection of Figure 9 reveals some structural differences between carbon black and diesel soot particles. For example, there were no pronounced features at $q \sim 0.3\text{ nm}^{-1}$ corresponding to primary particles (level 3). Thus, $R_{g,3}$ was assumed to be similar to that of carbon black (14 nm; see Table 2), and this parameter was held constant during data fitting. SAXS analysis showed that the radius of gyration of the soot aggregates, $R_{g,2} = 37\text{ nm}$ (Table 2, level 2), which corresponds to a mean particle diameter of 57 nm ($2R_{g,2}(3/5)^{1/2}$), is significantly smaller than that calculated for the carbon black aggregates. This result is consistent with TEM observations and DLS data. The power law exponent, P_2 , for these aggregates is 3.8. This value is quite similar to that of carbon black (see Table 2), suggesting a comparable degree of surface roughness for the diesel soot primary particles. The power law exponent for the mass fractals formed by the aggregates (Table 2, level 1) corresponds to a fractal dimension of 2.1. Thus, compared to the carbon black particles, the structural morphology of the soot particles dispersed in *n*-dodecane can be described as relatively loose mass fractals. This conclusion is also supported by TEM studies (see Figure 1).

SAXS patterns indicate that addition of either dOCP or PS-PEP has a similar effect on the hierarchical structure of both carbon black and diesel soot particles. In all cases, the characteristic mass fractal dimension, P_1 , is significantly reduced (see Table 2), suggesting that the addition of either copolymer transforms the initially compact agglomerates into relatively loose aggregates. In the case of dOCP, the mean size of the carbon black aggregates is also reduced. There is also a discernible increase in the power law exponent for the aggregates, P_2 , from 3.8 up to 4.2 (see Table 2). This suggests copolymer adsorption, since copolymer chains of relatively low electron density coating relatively high electron density carbon black aggregates is expected to produce a diffuse interface between the aggregates and the surrounding environment. This leads to a negative deviation from Porod's law, for which the scattering intensity gradient is normally equal to -4.0 . SAXS analysis of the carbon black also confirms that the primary particle size remains approximately 14 nm, with insignificant deviations in the other parameters associated with this structural level. Thus, addition of either dOCP or PS-PEP to the carbon black does not affect the structure of its primary particles. It is assumed that this is also the case for diesel soot.

CONCLUSIONS

In summary, certain grades of carbon black, such as the one studied herein, can be useful mimics for understanding the behavior of specific types of diesel soot. These two colloidal substrates can possess rather similar fractal morphologies, grain sizes, and densities. Moreover, the extent of copolymer

adsorption behavior may be reasonably comparable, despite discernible differences in surface elemental composition for these two substrates.

SAXS can be used to assess the various hierarchical structures of both carbon black and diesel soot. For example, the mean radius of gyration determined for soot aggregates is significantly smaller than that calculated for carbon black aggregates. In the absence of any copolymer, soot particle suspensions in *n*-dodecane comprise relatively loose mass fractals compared to the corresponding carbon black suspensions. SAXS also provides evidence for copolymer adsorption and indicates that addition of either copolymer transforms the initially compact agglomerates into relatively loose aggregates. Based on SAXS analysis, addition of either dOCP or PS-PEP to the carbon black does not significantly affect the structure of its primary particles. It is believed that this is also the case for diesel soot.

In favorable cases, remarkably similar experimental data can be obtained for carbon black and diesel soot when using dOCP and PS-PEP as copolymer dispersants. However, it is not difficult to identify certain copolymer-particle-solvent combinations for which substantial differences can be observed. Such observations are most likely the result of dissimilar surface chemistries, which can have a profound effect on the colloidal stability.

ASSOCIATED CONTENT

Supporting Information

The Supporting Information is available free of charge on the ACS Publications website at DOI: 10.1021/acs.langmuir.5b02017.

XPS C 1s core-line spectra of carbon black and diesel soot, DLS particle size distributions for Regal 250R carbon black, and diesel soot suspensions in *n*-dodecane, thermogravimetric curves obtained for carbon black and diesel soot alone, plus each substrate coated with increasing amounts of dOCP or PS-PEP, isotherms obtained for dOCP or PS-PEP adsorbed onto diesel soot from *n*-dodecane at 20 °C determined indirectly by UV spectroscopy and directly by thermogravimetric analysis, summary table of copolymer adsorption data (PDF)

AUTHOR INFORMATION

Corresponding Author

*E-mail s.p.armes@shef.ac.uk (S.P.A.).

Notes

The authors declare no competing financial interest.

ACKNOWLEDGMENTS

BP Formulated Products Technology is thanked for funding a PhD studentship for D.J.G. Dr. D. Fomitchev (Cabot Corporation, Billerica, MA) is thanked for the donation of the Regal 250R carbon black.

REFERENCES

- (1) Lloyd, A. C.; Cackette, T. A. *J. Air Waste Manage. Assoc.* **2001**, *51*, 809.
- (2) Nehmer, D. R. R. SAE Technical Paper 1994, 940668.
- (3) Pope, C. A.; Thun, M. J.; Namboodiri, M. M.; Dockery, D. W.; Evans, J. S.; Speizer, F. E.; Heath, C. W. *Am. J. Respir. Crit. Care Med.* **1995**, *151*, 669.
- (4) Matti Maricq, M. *J. Aerosol Sci.* **2007**, *38*, 1079.
- (5) Kittelson, D. B. *J. Aerosol Sci.* **1998**, *29*, 575.
- (6) Virtanen, A. K. K.; Ristimäki, J. M.; Vaaraslahti, K. M.; Keskinen, J. *Environ. Sci. Technol.* **2004**, *38*, 2551.

- (7) Shank, G.; Goshorn, K.; Cooper, M.; Van Dam, W.; Richards, S. A history of mack engine lubricant tests from 1985–2005: Mack T-7 through mack T-12, SAE Technical Paper, 2005-01-3713.
- (8) Kinker, B.; Fischer, M.; Bollinger, M.; Cybert, R.; Bielmeier, E.; Cooper, D.; Fischer, A.; Croessmann, M. US, 2009.
- (9) Maiboom, A.; Tauzia, X.; Hétet, J.-F. *Energy* **2008**, *33*, 22.
- (10) Zheng, M.; Reader, G. T.; Hawley, J. G. *Energy Convers. Manage.* **2004**, *45*, 883.
- (11) Abd-Alla, G. H. *Energy Convers. Manage.* **2002**, *43*, 1027.
- (12) Cadman, W. J. J. SAE Technical Paper 1986, 860378.
- (13) Ladommato, N.; Balian, R.; Horrocks, R.; Cooper, L. SAE Technical Paper 1996, 960841.
- (14) Selby, K. Rheology of soot thickened diesel engine oils, SAE Technical Paper, 1998, 981369.
- (15) Kuo, C. C.; Passut, C. A.; Jao, T.-C.; Csontos, A. A.; Howe, J. M. Wear mechanism in Cummins M-11 high soot diesel test engines, SAE Technical Paper, 1998, 981372.
- (16) Devlin, M. T.; Li, S.; Burgess, T.; Jao, T.-C. Film formation properties of polymers in the presence of abrasive contaminants, SAE Technical Paper, 2002-01-2793.
- (17) Li, S.; Csontos, A. A.; Gable, B. M.; Passut, C. A.; Jao, T.-C. Wear in Cummins M-11/EGR test engines, SAE Technical Paper, 2002-01-1672.
- (18) Gautam, M.; Chitoor, K.; Durbha, M.; Summers, J. C. *Tribol. Int.* **1999**, *32*, 687.
- (19) Green, D. A.; Lewis, R. *Proc. Inst. Mech. Eng., Part D* **2008**, *222*, 1669.
- (20) Zheng, R.; Liu, G.; Devlin, M.; Hux, K.; Jao, T. *Tribol. Trans.* **2009**, *53*, 97.
- (21) Diatto, P.; Anzani, M.; Tinucci, L.; Tripaldi, G.; Vettor, A. *Tribol. Ser.* **1999**, *36*, 809.
- (22) Shar, J. A.; Cosgrove, T.; Obey, T. M.; Warne, M. R.; Wedlock, D. *J. Langmuir* **1999**, *15*, 7688.
- (23) Bartha, L.; Deák, Y. G.; Hancsók, J.; Baladincz, J.; Auer, J.; Kocsis, Z. *Lubr. Sci.* **2001**, *13*, 313.
- (24) Kozak, D.; Moreton, D.; Vincent, B. *Colloids Surf., A* **2009**, *347*, 245.
- (25) Hu, E.; Hu, X.; Liu, T.; Fang, L.; Dearn, K. D.; Xu, H. *Wear* **2013**, *304*, 152.
- (26) Smiechowski, M. F.; Lvovich, V. F. *J. Electroanal. Chem.* **2005**, *577*, 67.
- (27) Clague, A. D. H.; Donnet, J. B.; Wang, T. K.; Peng, J. C. M. *Carbon* **1999**, *37*, 1553.
- (28) Pahalagedara, L.; Sharma, H.; Kuo, C.-H.; Dharmarathna, S.; Joshi, A.; Suib, S. L.; Mhadeshwar, A. B. *Energy Fuels* **2012**, *26*, 6757.
- (29) Bezot, P.; Hesse-Bezot, C.; Rousset, B.; Diraison, C. *Colloids Surf., A* **1995**, *97*, 53.
- (30) Bezot, P.; Hesse-Bezot, C.; Diraison, C. *Carbon* **1997**, *35*, 53.
- (31) Müller, J. O.; Su, D. S.; Jentoft, R. E.; Wild, U.; Schlägl, R. *Environ. Sci. Technol.* **2006**, *40*, 1231.
- (32) Müller, J.-O.; Su, D. S.; Wild, U.; Schlägl, R. *Phys. Chem. Chem. Phys.* **2007**, *9*, 4018.
- (33) Gowney, D. J.; Mykhaylyk, O. O.; Armes, S. P. *Langmuir* **2014**, *30*, 6047.
- (34) Ilavsky, J.; Jemian, P. R. *J. Appl. Crystallogr.* **2009**, *42*, 347.
- (35) Scares, B. G.; de Souza Gomes, A. *Polym. Bull.* **1988**, *20*, 543.
- (36) Gowney, D. J.; Mykhaylyk, O. O.; Derouineau, T.; Fielding, L. A.; Smith, A. J.; Aragrag, N.; Lamb, G. D.; Armes, S. P. *Macromolecules* **2015**, *48*, 3691.
- (37) Watts, J. F. *Vacuum* **1994**, *45*, 653.
- (38) Kirchner, U.; Vogt, R.; Natzeck, C.; Goschnick, J. *J. Aerosol Sci.* **2003**, *34*, 1323.
- (39) Swartz, W. E. *Anal. Chem.* **1973**, *45*, 788A.
- (40) Scares, B.; de Souza Gomes, A. *Polym. Bull.* **1988**, *20*, 543.
- (41) Choi, S.-H.; Bates, F. S.; Lodge, T. P. *J. Phys. Chem. B* **2009**, *113*, 13840.
- (42) Quintana, J. R.; Villacampa, M.; Katime, I. A. *Macromolecules* **1993**, *26*, 606.
- (43) Cohen Stuart, M. A.; Cosgrove, T.; Vincent, B. *Adv. Colloid Interface Sci.* **1985**, *24*, 143.
- (44) Pirouz, S.; Duhamel, J.; Jiang, S.; Duggal, A. *Macromolecules* **2015**, *48*, 4620.
- (45) Rieker, T. P.; Misono, S.; Ehrburger-Dolle, F. *Langmuir* **1999**, *15*, 914.
- (46) Won, Y.-Y.; Meeker, S. P.; Trappe, V.; Weitz, D. A.; Diggs, N. Z.; Emerit, J. I. *Langmuir* **2005**, *21*, 924.
- (47) Lerche, D.; Sobisch, T. *Powder Technol.* **2007**, *174*, 46.
- (48) Detloff, T.; Sobisch, T.; Lerche, D. *Powder Technol.* **2007**, *174*, 50.
- (49) Detloff, T.; Sobisch, T.; Lerche, D. *Particle & Particle Systems Characterization* **2006**, *23*, 184.
- (50) Gowney, D. J.; Fowler, P. W.; Fielding, L. A.; Mykhaylyk, O. O.; Derry, M. J.; Aragrag, N.; Lamb, G. D.; Armes, S. P. *Langmuir* **2015**, *31*, 8764.
- (51) Braun, A.; Huggins, F. E.; Seifert, S.; Ilavsky, J.; Shah, N.; Kelly, K. E.; Sarofim, A.; Huffman, G. P. *Combust. Flame* **2004**, *137*, 63.
- (52) di Stasio, S.; Mitchell, J. B. A.; LeGarrec, J. L.; Biennier, L.; Wulff, M. *Carbon* **2006**, *44*, 1267.
- (53) Hessler, J. P.; Seifert, S.; Winans, R. E.; Fletcher, T. H. *Faraday Discuss.* **2001**, *119*, 395.
- (54) Koga, T.; Hashimoto, T.; Takenaka, M.; Aizawa, K.; Amino, N.; Nakamura, M.; Yamaguchi, D.; Koizumi, S. *Macromolecules* **2008**, *41*, 453.
- (55) Sorensen, C. M.; Oh, C.; Schmidt, P. W.; Rieker, T. P. *Phys. Rev. E: Stat. Phys., Plasmas, Fluids, Relat. Interdiscip. Top.* **1998**, *58*, 4666.
- (56) Koga, T.; Takenaka, M.; Aizawa, K.; Nakamura, M.; Hashimoto, T. *Langmuir* **2005**, *21*, 11409.
- (57) Rieker, T. P.; Hindermann-Bischoff, M.; Ehrburger-Dolle, F. *Langmuir* **2000**, *16*, 5588.
- (58) Braun, A.; Ilavsky, J.; Seifert, S.; Jemian, P. R. *J. Appl. Phys.* **2005**, *98*, 073513.
- (59) Beauchage, G. *J. Appl. Crystallogr.* **1995**, *28*, 717.
- (60) Beauchage, G. *J. Appl. Crystallogr.* **1996**, *29*, 134.
- (61) Beauchage, G.; Schaefer, D. W. *J. Non-Cryst. Solids* **1994**, *172*, 797.
- (62) Braun, A.; Shah, N.; Huggins, F. E.; Kelly, K. E.; Sarofim, A.; Jacobsen, C.; Wirick, S.; Francis, H.; Ilavsky, J.; Thomas, G. E.; Huffman, G. P. *Carbon* **2005**, *43*, 2588.
- (63) Beauchage, G.; Ulibarri, T. A.; Black, E. P.; Schaefer, D. W. In *Hybrid Organic-Inorganic Composites*, 1995; Vol. 585, p 97; doi 10.1021/bk-1995-0585.ch009.